Research Article | Vol. 25, No. 17 | 21 Aug 2017 | OPTICS EXPRESS 20466
Optics EXPRESS

Optimization of nano-honeycomb structures for flexible w-LEDs

HUANG-YU LIN,[1] YUNG-MIN PAI,[1] JING-XING SHI,[2] XIN-YIN CHEN,[1] CHUNG-HSIANG LIN,[1] CHIH-MING WENG,[1] TZU-YU CHEN,[1] CHIEN-CHUNG LIN,[3] MARTIN DAVID BRIAN CHARLTON,[2] YI-PAI HUANG,[1] CHYONG-HUA CHEN,[1] HUANG-MING PHILIP CHEN,[1] AND HAO-CHUNG KUO[1,*]

[1]*Department of Photonics and Institute of Electro-Optical Engineering, National Chiao Tung University, Hsinchu 30010, Taiwan*
[2]*School of Electronics and Computer Science, University of Southampton, Southampton SO171BJ, UK*
[3]*Institute of Photonic System, National Chiao Tung University, Tainan 711, Taiwan*
[*]*hckuo@faculty.nctu.edu.tw*

Abstract: This study presents the low cost fabrication of flexible white-light-emitting diodes (w-LEDs) with nano-honeycomb-structured phosphor films. Extending the dimensions of the nano-honeycomb structures improved the color uniformity of the flexible samples, and the 950-nm pattern sample demonstrated optimal color uniformity because this nano-pattern exhibited an excellent diffusion ability owing to its pitch size. In addition to color uniformity, the use of this nano-pattern improved the luminous efficiency. The 750-nm pattern exhibited the highest luminous efficiency (235.8 lm/W), which was approximately 7% higher than that exhibited by a non-patterned phosphor film sample. Thus, flexible w-LEDs with nano-honeycomb structure optimization have great potential to be used as next-generation lighting sources.

OCIS codes: (230.3670) Light-emitting diodes; (230.2090) Electro-optical devices; (050.5298) Photonic crystals.

References and links

1. Y. Narukawa, M. Sano, M. Ichikawa, S. Minato, T. Sakamoto, T. Yamada, and T. Mukai, "Improvement of luminous efficiency in white light emitting diodes by reducing a forward-bias voltage," Jpn. J. Appl. Phys. **46**(40), L963–L965 (2007).
2. S. Nakamura, T. Mukai, and M. Senoh, "Candela-class high-brightness InGaN/AlGaN double-heterostructure blue-light-emitting diodes," Appl. Phys. Lett. **64**(13), 1687–1689 (1994).
3. E. F. Schubert and J. K. Kim, "Solid-state light sources getting smart," Science **308**(5726), 1274–1278 (2005).
4. D. A. Steigerwald, J. C. Bhat, D. Collins, R. M. Fletcher, M. O. Holcomb, M. J. Ludowise, P. S. Martin, and S. L. Rudaz, "Illumination with solid state lighting technology," IEEE J. Sel. Top. Quantum Electron. **8**(2), 310–320 (2002).
5. J. K. Kim, H. Luo, E. F. Schubert, J. Cho, C. Sone, and Y. Park, "Strongly enhanced phosphor efficiency in GaInN white light-emitting diodes using remote phosphor configuration and diffuse reflector cup," Jpn. J. Appl. Phys. **44**(21), L649–L651 (2005).
6. J. H. Ahn, H. S. Kim, K. J. Lee, S. Jeon, S. J. Kang, Y. Sun, R. G. Nuzzo, and J. A. Rogers, "Heterogeneous three-dimensional electronics by use of printed semiconductor nanomaterials," Science **314**(5806), 1754–1757 (2006).
7. M. A. Meitl, Z. T. Zhu, V. Kumar, K. J. Lee, X. Feng, Y. Y. Huang, I. Adesida, R. G. Nuzzo, and J. A. Rogers, "Transfer printing by kinetic control of adhesion to an elastomeric stamp," Nat. Mater. **5**(1), 33–38 (2006).
8. L. Wang, J. Ma, Z. Liu, X. Yi, H. Zhu, and G. Wang, "In situ fabrication of bendable microscale hexagonal pyramids array vertical light emitting diodes with graphene as stretchable electrical interconnects," ACS Photonics **1**(5), 421–429 (2014).
9. H. V. Han, H. Y. Lin, C. C. Lin, W. C. Chong, J. R. Li, K. J. Chen, P. Yu, T.-M. Chen, H.-M. Chen, K.-M. Lau, and H. C. Kuo, "Resonant-enhanced full-color emission of quantum-dot-based micro LED display technology," Opt. Express **23**(25), 32504–32515 (2015).
10. T. Nakayama, K. Hiyama, K. Furukawa, and H. Ohtani, "Development of phosphorescent white OLED with high power efficiency and long lifetime," Konica Minolta Technology Report **5**, 115 (2008).
11. R. H. Kim, S. Kim, Y. M. Song, H. Jeong, T. I. Kim, J. Lee, X. Li, K. D. Choquette, and J. A. Rogers, "Flexible vertical light emitting diodes," Small **8**(20), 3123–3128 (2012).

#291084 https://doi.org/10.1364/OE.25.020466
Journal © 2017 Received 21 Mar 2017; revised 6 May 2017; accepted 7 May 2017; published 14 Aug 2017

Optics EXPRESS

12. Y. Sun and J. A. Rogers, "Inorganic semiconductors for flexible electronics," Adv. Mater. **19**(15), 1897–1916 (2007).
13. T. i. Kim, S. Hyun Lee, Y. Li, Y. Shi, G. Shin, S. Dan Lee, Y. Huang, J. A. Rogers, and J. Su Yu, "Temperature- and size-dependent characteristics in ultrathin inorganic light-emitting diodes assembled by transfer printing," Appl. Phys. Lett. **104**(5), 051901 (2014).
14. J. G. McCall, T. I. Kim, G. Shin, X. Huang, Y. H. Jung, R. Al-Hasani, F. G. Omenetto, M. R. Bruchas, and J. A. Rogers, "Fabrication and application of flexible, multimodal light-emitting devices for wireless optogenetics," Nat. Protoc. **8**(12), 2413–2428 (2013).
15. S. Xu, Y. Zhang, J. Cho, J. Lee, X. Huang, L. Jia, J. A. Fan, Y. Su, J. Su, H. Zhang, H. Cheng, B. Lu, C. Yu, C. Chuang, T. I. Kim, T. Song, K. Shigeta, S. Kang, C. Dagdeviren, I. Petrov, P. V. Braun, Y. Huang, U. Paik, and J. A. Rogers, "Stretchable batteries with self-similar serpentine interconnects and integrated wireless recharging systems," Nat. Commun. **4**, 1543 (2013).
16. D. Feng, Y. Yan, X. Yang, G. Jin, and S. Fan, "Novel integrated light-guide plates for liquid crystal display backlight," J. Opt. A, Pure Appl. Opt. **7**(3), 111–117 (2005).
17. P. H. Huang, T. C. Huang, Y. T. Sun, and S. Y. Yang, "Large-area and thin light guide plates fabricated using UV-based imprinting," Opt. Express **16**(19), 15033–15038 (2008).
18. C. W. Sher, K. J. Chen, C. C. Lin, H. V. Han, H. Y. Lin, Z. Y. Tu, H. H. Tu, K. Honjo, H.-Y. Jiang, S. L. Ou, R. H. Horng, X. Li, C. C. Fu, and H. C. Kuo, "Large-area, uniform white light LED source on a flexible substrate," Opt. Express **23**(19), A1167–A1178 (2015).
19. C. Y. Liu, K. J. Chen, D. W. Lin, C. Y. Lee, C. C. Lin, S. H. Chien, M. H. Shih, G. C. Chi, C. Y. Chang, and H.-C. Kuo, "Improvement of emission uniformity by using micro-cone patterned PDMS film," Opt. Express **22**(4), 4516–4522 (2014).
20. H. Y. Lin, S. W. Wang, C. C. Lin, Z. Y. Tu, P. T. Lee, H. M. Chen, and H. C. Kuo, "Effective optimization and analysis of white LED properties by using nano-honeycomb patterned phosphor film," Opt. Express **24**(17), 19032–19039 (2016).
21. G. Widawski, M. Rawiso, and B. François, "Self-organized honeycomb morphology of star-polymer polystyrene films," (1994).
22. J. Zhao, A. Wang, M. A. Green, and F. Ferrazza, "19.8% efficient "honeycomb" textured multicrystalline and 24.4% monocrystalline silicon solar cells," Appl. Phys. Lett. **73**(14), 1991–1993 (1998).
23. L. A. Connal and G. G. Qiao, "Preparation of Porous Poly (dimethylsiloxane)-Based Honeycomb Materials with Hierarchal Surface Features and Their Use as Soft-Lithography Templates," Adv. Mater. **18**(22), 3024–3028 (2006).
24. H. T. Chiu, C. Y. Chang, C. L. Chen, T. Y. Chiang, and M. T. Guo, "Preparation and characterization of UV-curable organic/inorganic hybrid composites for NIR cutoff and antistatic coatings," J. Appl. Polym. Sci. **120**(1), 202–211 (2011).
25. C. C. Lin, W. L. Liu, and C. Y. Hsieh, "Scalar scattering model of highly textured transparent conducting oxide," J. Appl. Phys. **109**(1), 014508 (2011).
26. H. Y. Lin, K. J. Chen, S. W. Wang, C. C. Lin, K. Y. Wang, J. R. Li, P. T. Lee, M. H. Shih, X. Li, H. M. Chen, and H. C. Kuo, "Improvement of light quality by DBR structure in white LED," Opt. Express **23**(3), A27–A33 (2015).
27. R. N. Shepard, "Attention and the metric structure of the stimulus space," J. Math. Psychol. **1**(1), 54–87 (1964).
28. I. Moreno and L. M. Molinar, "Color uniformity of the light distribution from several cluster configurations of multicolor LEDs," in *Optics & Photonics 2005*(International Society for Optics and Photonics, 2005), pp. 59411S–59411S–59417.
29. B. Y. Joo and J. H. Ko, "Analysis of color uniformity of white LED lens packages for direct-lit LCD backlight applications," J. Opt. Soc. Korea **17**(6), 506–512 (2013).
30. T. F. Krauss, "Slow light in photonic crystal waveguides," J. Phys. D Appl. Phys. **40**(9), 2666–2670 (2007).
31. H. T. Chiu, C. Y. Chang, C. L. Chen, T. Y. Chiang, and M. T. Guo, "Preparation and characterization of UV-curable organic/inorganic hybrid composites for NIR cutoff and antistatic coatings," J. Appl. Polym. Sci. **120**(1), 202–211 (2011).
32. Y. L. Tsai, C. Y. Liu, C. Krishnan, D. W. Lin, Y. C. Chu, T. P. Chen, T. L. Shen, T. S. Kao, M. D. Charlton, P. Yu, C. C. Lin, H. C. Kuo, and J. H. He, "Bridging the "green gap" of LEDs: giant light output enhancement and directional control of LEDs via embedded nano-void photonic crystals," Nanoscale **8**(2), 1192–1199 (2016).
33. J. Y. Chen, W. L. Chang, C. K. Huang, and K. W. Sun, "Biomimetic nanostructured antireflection coating and its application on crystalline silicon solar cells," Opt. Express **19**(15), 14411–14419 (2011).
34. C. K. Huang, K. W. Sun, and W. L. Chang, "Efficiency enhancement of silicon solar cells using a nano-scale honeycomb broadband anti-reflection structure," Opt. Express **20**(1), A85–A93 (2012).

1. Introduction

White-emitting diodes (w-LEDs) have become more common and indispensable in recent years. LEDs are manufactured using green technology and expected to replace conventional incandescent light bulbs [1–3]. The main approach for manufacturing white-light packages is based on yttrium aluminum garnet (YAG) phosphor and gallium nitride–based blue chips,

Optics EXPRESS

and the most common phosphor packages for fabricating w-LEDS are as follows: phosphor dispensing, conformal phosphor [4], and remote phosphor packages [5]. Solid-state lighting devices such as LEDs were previously used for lighting, signal, and display applications; however, their use is limited nowadays. To further extend their application, flexible LEDs have been developed for wearable displays, lighting, and biomedicine [6–8].

Organic LEDs (OLEDs) are among the excellent candidates for flexible devices. OLEDs are more widely used because of the excellent color quality and surface thinness, which makes them flexible and thus suitable for flexible lighting and displays. However, OLEDs cannot be used for common flexible lighting because of challenges such as low reliability and efficiency, short lifespan, and high cost [9,10]. Therefore, inorganic flexible LEDs with higher efficiency than that of OLEDs should be developed.

Rogers *et al*. extensively investigated flexible devices as the prospective technology for flexible lighting. Specialized semiconductor layer epitaxy, micro-scale LED chips, transfer printing technology, and systematic analysis in nanoscale for related systems have been used for fabricating flexible devices [11–15]. However, these technologies are complicated, thus making the manufacturing of flexible devices difficult. The most common approach is to develop bending lighting by combining solid-state lighting and the curved light guide [16,17]. However, the light guide plate is too hard and could not be freely bent many times, thus making it unsuitable for most flexible applications. In our study, we developed a considerably easier approach for fabricating flexible lighting by using a flip chip, silicone-based anisotropic conductive adhesive, and phosphor film [18].

To optimize w-LEDs, a textured polydimethylsiloxane (PDMS) pattern was transferred using a patterned sapphire structure. The textured phosphor film was used to improve the color uniformity of w-LEDs in [19]. However, the textured film does not enhance luminous efficiency. Therefore, a nano-honeycomb-structured phosphor film was investigated to not only improve the luminous efficiency but also optimize the color uniformity of w-LEDs [20]. In the present study, a patterned phosphor was employed to optimize flexible w-LEDs by using nano-honeycomb patterned phosphor films and improve the efficiency and uniformity. The nano-honeycomb structure has been fabricated by several research groups by using any approaches which were determined for any applications [21,22]. The transfer printing method is widely used for fabricating nano-honeycomb structures, in which a nano-honeycomb film is developed by pouring dilute benzene solution of a star polymer onto a glass surface [23].

2. Experimental methods

The experiment in this study involved two steps: fabrication of the blue-flip-chip–based flexible substrate and the manufacture of the nano-honeycomb phosphor film combined with the flexible substrate to produce flexible w-LEDs. Figure 1(a) presents the layout of the flexible substrate with the electrode, with the area of the electrode defined by wet etching and photolithography and coated with 30-μm bonding adhesive to facilitate adhesion of the metal electrode on the substrate. Subsequently, the substrate was coated with a 30-μm-thick copper stripe by using an e-gun machine. As shown in the inset, the gap between the bonded anode and cathode pads was set as approximately 100 μm. Figure 1(b) presents the bonding of the flexible substrate with the 3x3 blue flip chips by using a silicon based anisotropic conductive adhesive (Dexerials Corporation) at a temperature of 230 °C and pressure of 22.5 kg for 180 s. The flip chip bonded on the flexible substrate process was referred from our past research [18]. Fig. 1 (d)-1(e) illustrates the nano honeycomb-structured phosphor film fabrication. First, nano-spheres with diameters of 1.2 μm, 1 μm, 600 nm, and 400 nm were prepared and coated onto the glass. Before the nano-sphere coated process, we mixed the PS nano-sphere with the DI-water and alcohol to produce the suspension solution, and then added to the aqueous solution with sodium dodecyl sulfate (SDS) as surfactant in order to produce the uniformity arrangement. Next, let the suspension solution floating on the DI-water and then coated onto the glass. Figure 2 (a) and 2(b) show that the SEM top view images of the PS

Optics EXPRESS

nano-sphere coated glass without the SDS treated, it seems to be un-uniformity. The more uniformity PS nano-sphere arrangement after the SDS treated was as shown in Fig. 2(c) and 2(d), it was suitable for the large area flexible white LED. Second, the PDMS suspension slurry was blended with 15 wt% YAG phosphor in silicone glue and then cast onto the nano-sphere coated glass substrate. After the glass substrate was baked at 70 °C for 10 min, the nano-honeycomb-structured phosphor film was combined with the blue-chip-based flexible substrate. Subsequently, the area of 5x5 cm flexible w-LEDs were covered with nano-honeycomb-structured patterned-up and patterned-down phosphor films.

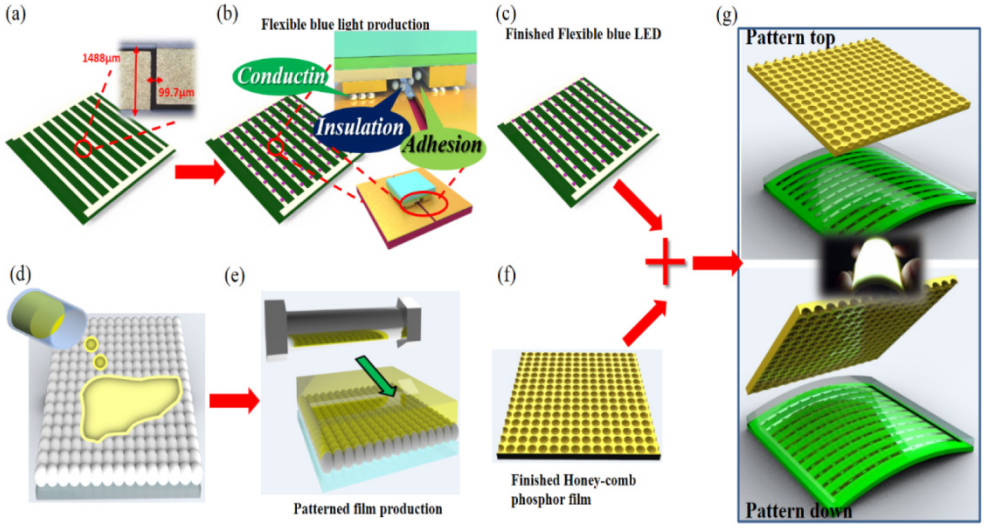

Fig. 1. Experiment flowchart. (a, b) Fabrication of the blue flip-chip-based flexible substrate by using an anisotropic conductive adhesive, and (d, e) honeycomb structure phosphor film fabrication. Flexible white-LEDs covered with (c) patterned-up and (f) patterned-down nano-honeycomb structure phosphor film.

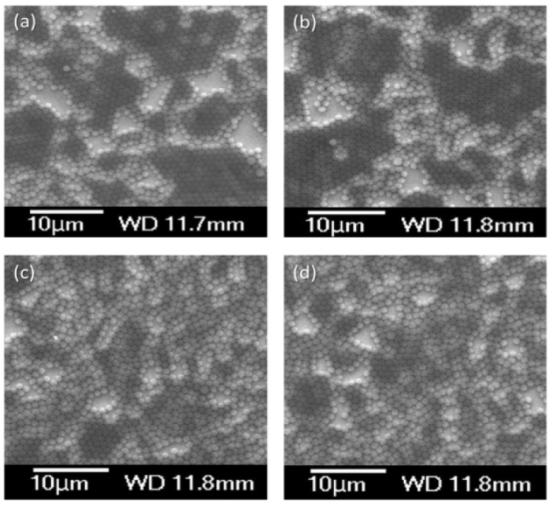

Fig. 2. (a)(b) The SEM top view images of the PS nano-sphere coated glass without the SDS treated and (c)(d) after the SDS treatment.

Figure 3 presents the top view and cross-sectional scanning electron microscopy images of nano-honeycomb-structured phosphor films of several dimensions. The phosphor films with 350- and 450-nm patterns were transferred by using polystyrene (PS) nano-spheres of

Optics EXPRESS

400 and 600 nm, respectively, and the depths of impression of these films were approximately 76 and 105 nm, respectively. PS nano-spheres of 1 and 1.2 μm could produce 750- and 950-nm patterns with impression depths of approximately 150 and 240 nm, respectively.

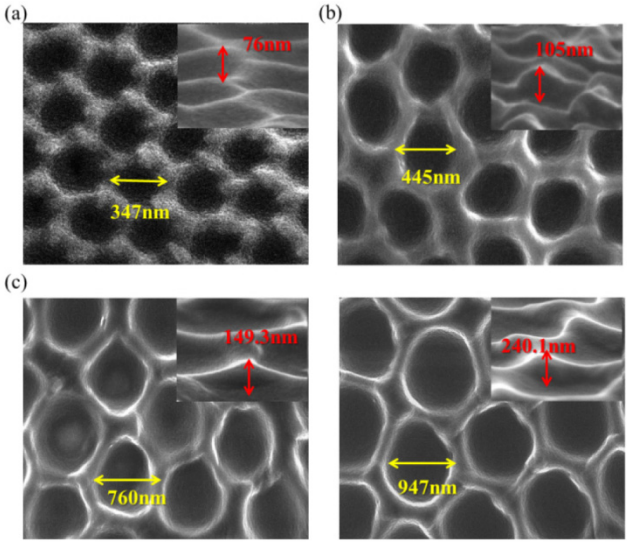

Fig. 3. SEM images of the honeycomb-patterned PDMS films with a dimension of (a) 350 nm, (b) 450 nm, (c) 750 nm, and (d) 950 nm.

3. Result and discussion

The diffusion ability of the nano-honeycomb structured phosphor film was investigated through haze measurement. Figure 4(a) and 4(b) presents the approaches of measuring total transmittance (total direct light transmission) and diffusion transmittance (excluding the normal direct light transmission) by using the U4100 system. The laser beam was passed through the phosphor film, which diffused in the integrating sphere, and the omnidirectional total transmittance (T_{total}) was determined using the detector. However, diffusion transmittance ($T_{diffuse}$) was determined by opening the hole of the sphere facing the sample, which allowed the dissipation of most normal rays.

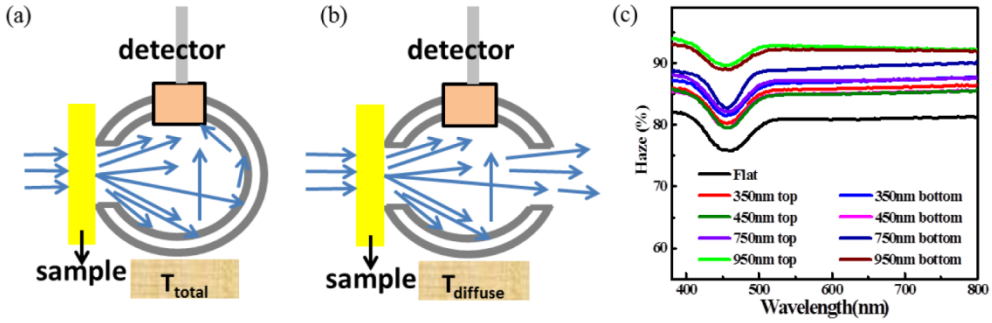

Fig. 4. Measurement of the (a) total transparence (total direct light transmission) and (b) diffusion transparence (excluding the normal direct light transmission) of the phosphor films. (c) The haze spectrum depends on the wavelength of the nano-honeycomb structured PDMS films with dimensions of 350, 450, 750, and 950 nm.

Figure 4(c) shows that the haze spectrum depends on the wavelength of the patterned phosphor film and is calculated as Eqs. (1) [24,25]:

Optics EXPRESS

$$\text{Haze}(\%) = \frac{T_{diffuse}}{T_{total}} 100\%. \quad (1)$$

Haze intensity is defined as the light scattering capability and is calculated as the ratio of diffracted photons and nonspecular photons when the rays pass through the patterned phosphor films. The haze value was improved by increasing the pitch size of the honeycomb structure, which contributed to the color uniformity optimization of the flexible w-LEDs. The 950-nm pattern yielded an excellent haze value, thus improving the diffusion ability.

This study investigated the influence of the dimension of the nano-honeycomb on color uniformity by using an SR-UL1R spectro-radiometer (TOPCON Corporation), as shown in Fig. 5(a). The color uniformities of the nano-honeycomb top pattern flexible samples with various pitch sizes are presented in Fig. 5. The area lighting samples with different dimensions of the nano-honeycomb structure were scanned to determine the maximum and minimum correlated color temperature (CCT), and the correlated chromaticity coordinates (u', v') of the maximum and minimum CCT were plotted [Fig. 5(b)–5(f)]. In these figures, the maximum CCTs always occurred in the middle of the blue chip because of the Lambertian pattern of blue rays [26]. The color uniformity of the area lighting source can be defined as the distance in color space (△u'v'), which was based on chromaticity coordinates (u', v') of the maximum and minimum CCT. The distance in color space (△u'v') can be calculated as Eqs. (2) [27–29]:

$$\Delta u'v'(x,y) = \sqrt{[u_1'(x,y) - u_2'(x,y)]^2 + [v_1'(x,y) - v_2'(x,y)]^2}. \quad (2)$$

By calculation, the △u'v' of the flat, 350-nm, 450-nm, 750-nm, and 950-nm honeycomb patterns for flexible LEDs was approximately 0.22758, 0.12295, 0.11447, 0.10721, and 0.10719, respectively. The lower distance in color space denoted the lower color separation, indicating that this property caused higher color uniformity [28].

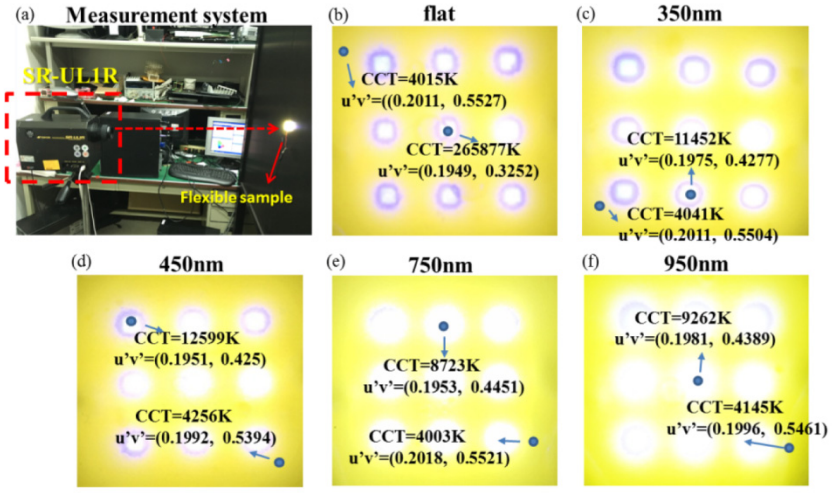

Fig. 5. (a) Chromaticity uniformity measurement system to investigate the uniformity of flexible samples by using an SR-UL1R spectro-radiometer. (b)–(f) Spots in the areas of the flexible LEDs depicting maximum and minimum correlated color temperature (CCT) and the correlated chromaticity coordinates have been analyzed to verify the color uniformity.

Figure 6 shows that the simulation mapping images to verify the influence for color uniformity of nano honeycomb by LightTools software, which was based on Mie scattering theory. We also calculated the distance in color space (△u'v') of the simulation result and the 950 nm was with the lower △u'v', which was similar to the experimental result. As the experimental and simulation results, indicated that increasing the pitch size of the nano-

Optics EXPRESS

honeycomb can improve color uniformity, and a nano-honeycomb structure sample with a pitch of 950 nm exhibited optimal color uniformity. When the light propagating in the phosphor film, coherently backscattered and omnidirectional reflection at each unit cell of the honeycomb structure, which was the main reason for the honeycomb structure to improve the color uniformity. Any blue rays coupling inside the phosphor film were changed the direct to the horizontal propagating direct and re-pumped the phosphor to improve the color uniformity [30].

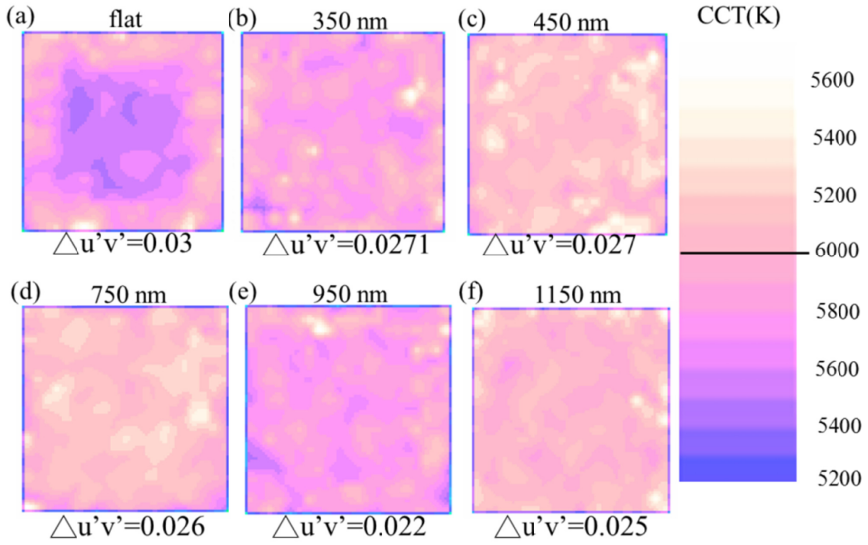

Fig. 6. Simulation of flexible w-LEDs to verify the influence of (a) flat phosphor film and the difference dimensions of (b) 350nm, (c) 450 nm, (d) 750 nm, (e) 950 nm, and (f) 1150 nm nano-honeycomb structure on color uniformity.

In addition to color uniformity, this study investigated the effect of the nano-honeycomb structure on luminous efficiency. The simulation emission spectra obtained using LightTools software at different dimensions of patterned top and bottom phosphor films of the flexible samples are presented in Fig. 7(a) and 7(b). The same concentration and the thickness of these phosphor films for the flexible samples were maintained, and modulating dimensions of the nano-honeycomb patterns yielded different luminous efficiency, as presented in Table 1. The 750-nm patterned-top phosphor film sample yielded the highest efficiency with an approximately 7% higher efficiency than the non-patterned phosphor film sample. Figure 7(c) presents the experimental emission spectra of flexible w-LEDs with different dimensions of the nano-honeycomb structure at a current of 120 mA. The suppression of blue rays and enhancement of yellow rays are illustrated in this figure, and the 750-nm pattern exhibited the strongest yellow band. The current-dependent luminous efficiencies of the flexible w-LEDs with various pitch sizes of the patterns are presented in Fig. 7(b). This study focused on the modulation of the nano-honeycomb structure to optimize flexible w-LEDs. Therefore, similar phosphor concentrations and thicknesses were maintained for several films to obtain similar yellow photon outputs. The luminous efficiencies of various samples are plotted in Table 2. The luminous efficiency of flexible w-LEDs with a nano-honeycomb pattern was higher than that of the flat phosphor film sample, and flexible w-LEDs with a 750-nm patterned top exhibited the highest luminous efficiency (7% higher than that of the flat phosphor sample). The experimental and simulation luminous efficiency results were consistent. The improvement in the efficiency was attributed to the nano-honeycomb pattern, which exhibited a high light extraction capability for flexible w-LEDs.

Optics EXPRESS

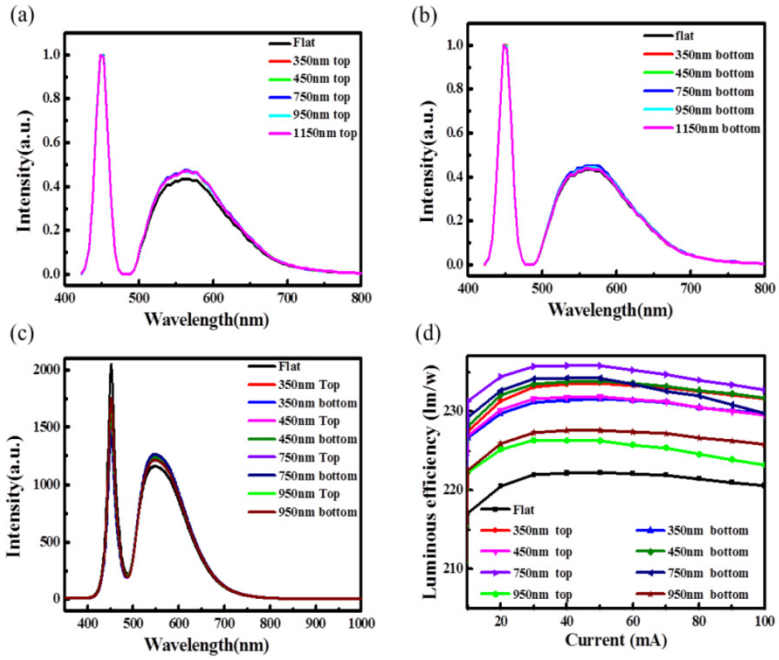

Fig. 7. Simulation emission spectra of the nano-honeycomb (a) patterned-up and (b) patterned-down phosphor films with dimensions of 350, 450, 750, 950, and 1150 nm for flexible LEDs. (c) Emission spectra of the flexible w-LEDs at a current of 120 mA and (d) luminous flux for the 360, 450, 750, and 950-nm nano-honeycomb patterned films covered with patterned top or bottom for the flexible w-LEDs.

Table 1. Simulation efficiency of flexible w-leds with various dimension patterns.

Type	Flat	350nm top	350nm bottom	450nm top	450nm bottom	750nm top
Efficiency(lm/w)	228.1	240	240	242.4	242.2	244
Type	750nm bottom	950nm top	950nm bottom	1150nm top	1150nm bottom	
Efficiency(lm/w)	243.9	238.2	237.6	236.7	236.1	

Table 2. experimental efficiency of flexible w-LEDs with various dimension patterns.

Type	Flat	350nm top	350nm bottom	450nm top	450nm bottom
Efficiency(lm/w)	218	229.6	229.4	231.7	231.5
Type	750nm top	750nm bottom	950nm top	950nm bottm	
Efficiency(lm/w)	233.1	233.1	226.4	226	

The measurement system detected reflection as a function of wavelength with various incident angles, as illustrated in Fig. 8(a) [31,32]. The reflections of the Lambertian blue ray from blue chips with different angles were analyzed using this system to verify the experiment results. The reflectance mapping image depended on different wavelengths and incident angles for the non-patterned phosphor films and various dimensions of nano-honeycomb patterned phosphor films, as shown in Fig. 8(b)–8(j). The mapping image of the flat sample indicates stronger reflectivity as a function of wavelength and incident angles, which indicates that most yellow photons will be reflected from the phosphor film, thus reducing light extraction. These figures illustrate that the yellow band had lower reflection for the patterned-top samples than for the non-patterned sample when the incident angle

Optics EXPRESS

extended, indicating that the nano-honeycomb pattern attributed to the photonic crystal property. The lowest reflectivity was observed in the 750-nm patterned-top phosphor film. The average reflection of blue rays for the 750 nm patterned sample is stronger than the flat, 350 nm, 450 nm patterned sample, which could induce the phosphor re-excited and improve the yellow band photons. On the other hand, the average reflection of yellow rays were lower than other patterned samples, it is the main reason to cause the 750-nm pattern exhibiting the best luminous efficiency. This result indicated that this dimension was induced the optimal light extraction, which was consistent with the experimentally obtained luminous efficiency results. The patterned phosphor films were as the antireflection (AR) layer to luminous efficiency of flexible white LEDs. The reason was that periodic nanostructures with gradient refractive indices become a sub-wavelength structure, the destructive interference have been occurred of the normal incident light at the particular wavelength and let abundant selected rays pass through the phosphor films [32]. K.W. Sun's group has investigated the nano-scale honeycomb structure to as the AR layer to improve the efficiency of the solar cell [33,34]. As the result, the patterned phosphor films is as the AR layer in this study and the luminous efficiency has been improved of our flexible w-LED.

In this study, the optimization of our flexible LEDs was contributed by the used of the nano honeycomb structure phosphor film. To analyze the effect of honeycomb structure phosphor film for the flexible LEDs, the ray tracing analysis of the individual blue LED element slitting simulation mode has been set up. The output photons comparison between the difference pitches of the honeycomb structures is shown in Fig. 9. From these simulation charts, the photons can be reflected back to re-pump the phosphors. The scattering can lead the resulting photons to the side and thus the color uniformity can be achieved. Meanwhile, when the yellow photons are generated more, the better luminous efficiency can be reached and the 750nm structure is better than other structures with different pitches.

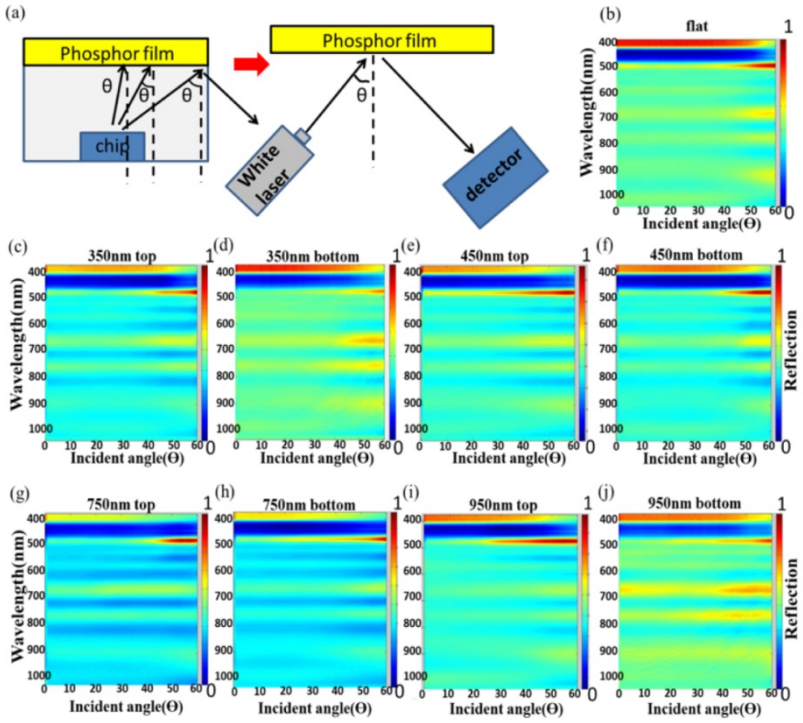

Fig. 8. (a) Angular dependence reflection measurement system for the patterned phosphor film. (b)–(i) Mapping images of normalized reflection as a function of wavelength with the incident angle for different dimensions of nano-honeycomb phosphor films.

Optics EXPRESS

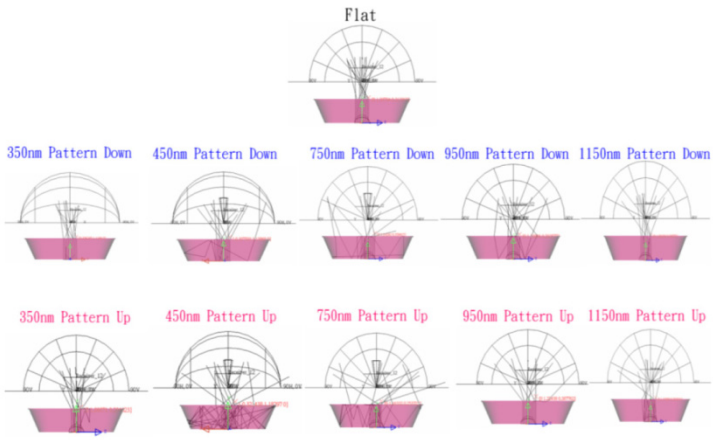

Fig. 9. The ray tracing simulation of the effect of the nano-honeycomb patterned for the flexible LEDs.

We demonstrated the nano-honeycomb structure phosphor film by the oversimplified approach to transfer the pattern by the PS nano-sphere. The Bending test system has been developed to verify the bending reliability of the flexible white LEDs as shown in Fig. 10. In the bending test, the flexible samples were bonded on the cylinder surface with difference diameters (*D*), the bending diameter was defined as shown in Fig. 10(a). Figure 10(b)-10(f) show that the performance of the patterned and non-patterned flexible LED under the bending condition. The best bending diameter of has been achieved about 10 mm for these flexible LED samples. The result indicated that the size variation of patterned phosphor films can't influence the bending ability of the flexible LEDs. We selected the best parameter of honeycomb patterned sample: 750 nm for the bending times test and compared to the reference sample (without pattern) as shown in Fig. 11. Figure 11(b) and 11(c) show that the bending times test with more times of bending circle of the non-patterned and 750 nm honeycomb patterned white flexible LED, respectively. The bending circles of these flexible LED samples were both below to 500 times. As the result, the nano-honeycomb patterned is located at the surface of the phosphor film and which does not affect the bending ability of the flexible LED.

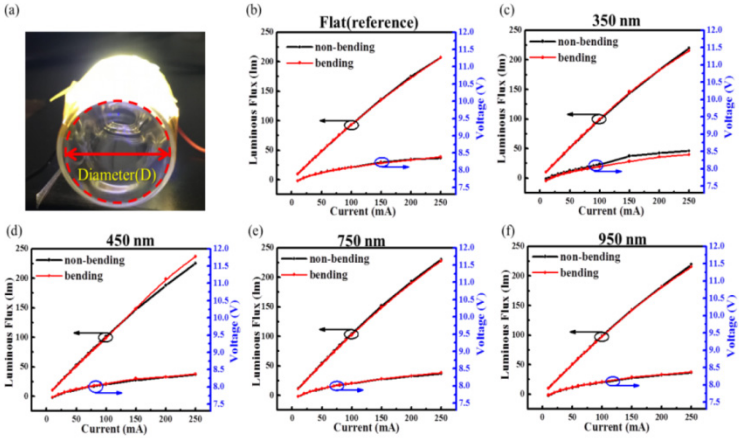

Fig. 10. (a) The bending diameter defined of bending test for flexible LEDs was illustrated in the picture. (b)-(f) The luminous flux and voltage of the flexible white LED of the non-patterned and difference size of honeycomb pattern flexible LEDs with the diameter of 10 mm bending test.

Optics EXPRESS

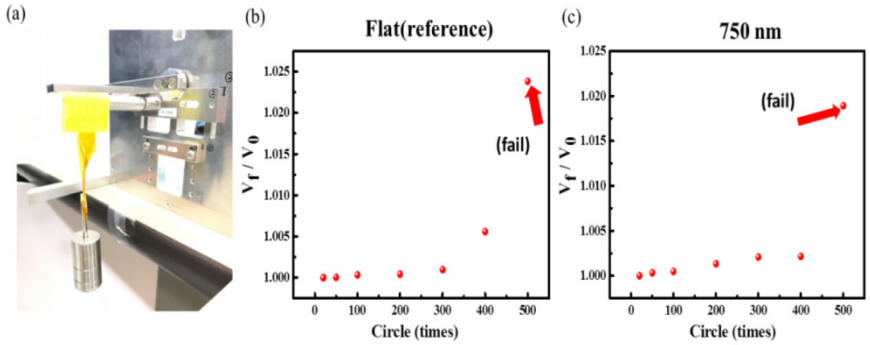

Fig. 11. (a) The image of the bending test measurement system for the difference size of patterned structure flexible LEDs. The bending test of (b) non-patterned and (c) 750 nm patterned samples are with more times of bending circle.

4. Conclusion

Nano honeycomb-structured phosphor films could improve the color uniformity and luminous efficiency of flexible w-LEDs. According to the angular dependence reflection measurement, the luminous efficiency improved because of the excellent light extraction. The 750-nm pattern exhibited the highest luminous efficiency, which was approximately 7% higher than that exhibited by the non-patterned phosphor film sample. In addition to luminous efficiency, nano-honeycomb structures could improve color uniformity to yield a higher haze value, which led to more efficient diffusion ability. This paper presents an easy approach to optimize flexible w-LEDs by using nanostructures of various dimensions. We believe that the incorporation of the nano-honeycomb structure into the flexible w-LEDs can be beneficial for the performance of the device.

Funding

Ministry of Science and Technology of Taiwan (MOST) grants (MOST105-2622-E-009-023-CC2, MOST104-3113-E-009-002-CC2).